FR9001309

COMMISSARIAT A L'ENERGIE ATOMIQUE
Centre d'Etudes Nucléaires de Saclay
91191 Gif-sur-Yvette Cedex

CEA - DPhPE 89-17
(LPC 89-24)
September 1989

Progress Report : Feasibility Study of an Indium Scintillator Solar Neutrino Experiment

A. de Bellefon
LPC, Collège de France, Paris

R. Barloutaud, A. Borg, J. Ernwein, L. Mosca
DPhPE Saclay, France

DEPARTEMENT DE PHYSIQUE DES PARTICULES ELEMENTAIRES

CEA - DPHPE -- 89-17

Progress Report : Feasibility Study of an Indium Scintillator Solar Neutrino Experiment

A. de Bellefon
LPC, Collège de France, Paris

R. Barloutaud, A. Borg, J. Ernwein, L. Mosca
DPhPE Saclay, France

Foreword

In this document, we report on the progress made in our attempt to demonstrate the feasibility of an experiment which would measure for the first time the two line sources of solar neutrinos resulting from electron capture by ^{7}Be and from the p-e-p reaction inside the sun. The detector under study consists of scintillator containing 10 tons of Indium .

This report is part of the studies performed within a working group of physicists from five countries[a]. This group has been meeting on a semi-annual schedule since September, 1988 to report on its work. The most recent meeting took place in September, 1989 at the Collège de France in Paris[b] and the results reported there are included in this document.

(a) The researchers of the working group belong to the following institutions:

1. ATT Bell Laboratories, USA
2. LPC, Collège de France, Paris
3. ISN, Grenoble, France
4. KEK, Nat. Lab. High Energy Phys., Japan
5. TU Munich, FRG
6. Oxford University, UK
7. University of Pennsylvania, USA
8. Queen Mary College, London, UK
9. DPhPE Saclay, France
10. ICCR, University of Tokyo, Japan

(b) Participants at this meeting were:

C. Beere, NE Technology, Edinburgh, UK, A. de Bellefon[2], N.E. Booth[6], R. Barloutaud[9], A. Borg[9], J.F. Cavaignac[3], J. Ernwein[9], F. von Feilitzsch[5], T. Inagaki[4], S.B. Kim[7], A.K. Mann[7], L. Mosca[9], R. Raghavan[1], G.L. Salmon[6], Y. Suzuki[10], J.C. Thevenin[9].

Contents

1. INTRODUCTION

Our working group is studying the feasibility of a solar neutrino experiment aimed at the real time measurement of the fluxes of the neutrino line sources from the reactions

$$e^- + {}^7Be \rightarrow {}^7Li + \nu_e \quad (862\ keV) \qquad (1)$$

and

$$p + e + p \rightarrow d + \nu_e \quad (1442\ keV) \qquad (2)$$

which take place in the sun.

The original proposal by R.S. Raghavan [1,1] to detect solar neutrinos through the inverse β-decay of indium

$$\nu_e + {}^{115}In \rightarrow {}^{115}Sn^* + e^- \qquad (3)$$

has been followed by attempts to design a detector capable of taking advantage of the unique properties of ^{115}In, namely its very low threshold (119 keV), and the fact that it is a nucleus with which a real time electronic experiment can measure the differential neutrino energy spectrum.

These attempts [1,2], [1,3] develop very finely segmented superconducting indium detectors to measure the low energy (0 - 420 keV) neutrinos from the most abundant source:

$$p + p \rightarrow d + e^+ + \nu_e \qquad (4)$$

These experiments are very difficult because the detectors are still in their infancy, and because the natural β^- radioactivity of ^{115}In (E_{max} = 494 keV) is a formidable background in this low energy region.

In this report we argue that an experiment capable of identifying by energy measurement the two line sources from electron capture by ^7Be (1) and from the p-e-p reaction (2) would be a very important contribution to our knowledge of neutrino properties and of our understanding of the sun as a neutrino source even without the measurement of the very low energy p-p neutrinos.

We calculate the expected detection efficiencies and event rates. We identify the backgrounds which must be overcome and we calculate the energy resolution which is needed and the radio-purity which must be achieved in the detector. Possible detector designs with techniques already used in particle physics are presented.

Finally, we list the necessary tests and developments which need to be made in order to check the feasibility of the experiment. These tests could be made in close connection with other "low background" experiments.

2. PHYSICS MOTIVATIONS

The solar neutrino problem arises from the fact that the ^{37}Cl experiment [2,1] finds about 1/3 of the neutrino rate predicted by what is generally accepted as a realistic model of the Sun, the Standard Solar Model (SSM) [2,2].

The consensus is that either we don't understand in detail the energy producing processes and dynamics of the Sun (and other stars), or that we have an incomplete understanding of the

physics of neutrinos. A commonly adopted view is that neutrinos have non-zero masses and that the electron-type neutrinos , ν_e , can undergo oscillations and change into the other types of neutrinos, ν_μ and ν_τ , which are undetectable in the ^{37}Cl experiment. Resonant oscillations in the Sun, the MSW effect [2,3], are a strong function of the mass differences of the various neutrino types, of the mixing angle, and of the neutrino energy. A detailed reanalysis of the SSM is in progress [2,4], and seems to indicate that the ^{8}B neutrino rate could be smaller than expected in the SSM. The predictions for low energy neutrinos from the more basic reactions in the sun are not changed.

It is important to point out that, because of its rather high neutrino energy threshold (814 keV), and because the neutrino capture cross section on ^{37}Cl is rising very rapidly with energy, the ^{37}Cl experiment is sensitive mainly to neutrinos from the decay of ^{8}B, which is produced rather high up in the chain of nuclear reactions. Its predicted rate in the Standard Solar Model is less certain than those of its precursors, the proton-proton fusion reaction and the interactions of ^{3}He and ^{4}He to produce ^{7}Be.

Clearly other experiments are needed, particularly those which are sensitive to the more basic processes, which produce neutrinos of much lower energy. Two new radiochemical experiments using ^{71}Ga as the target are in preparation, GALLEX [2,5] in the Gran Sasso laboratory in Italy, and SAGE [2,6] in the Baksan laboratory in the U.S.S.R. Other experiments are proposed to detect the ^{8}B neutrinos with even larger detectors and to detect them in real time. Recently the KAMIOKANDE water Cerenkov detector in Japan [2,7], originally designed to search for proton decay, has reported evidence for the detection of ^{8}B neutrinos at a level consistent with the ^{37}Cl experiment. This experiment, however, is only sensitive to the very high end of the ^{8}B spectrum, above 9 MeV and possibly ≈7.5 MeV in the future.

Because of the possibility that the solar neutrino problem is, at least in part, due to strongly energy dependent resonant oscillations, it is rather doubtful that radiochemical experiments can give us the complete answer. Some of the new proposed experiments, such as BOREX [2,8], a scintillation detector using a ^{11}B target, and SNO, a heavy water Cerenkov detector [2,9], will be able to measure the energy spectrum of the higher energy ^{8}B neutrinos. The only detector which can measure the energy spectrum of the more prolific lower energy neutrinos is one based on ^{115}In. In the experiment studied here we make no attempt to detect the very low energy p-p neutrinos, but concentrate on the monoenergetic neutrino lines at 862 keV, from electron capture in ^{7}Be, and at 1442 keV from the p-e-p reaction. Fig. 2.1 shows the energy range in which present and future solar neutrino experiments are sensitive.

For a detector containing 10 metric tons of indium we expect about 180 interactions per year from electron capture in ^{7}Be. This is a very important signal. In addition, it would also help interpreting the results of the present experiments. This is a crucial point because the MSW effect causes possible neutrino oscillations to be energy dependent in a complex way, and so the gallium experiments can no longer be expected to give a definite answer to the solar neutrino problem.

The detection rate for the p-e-p and ^8B neutrinos is much lower (≈ 13 and 24 interactions per year for 10 tons of indium respectively). However it is important to note that the intensity of the p-e-p line is directly proportional to the p-p fusion rate [2,10].

Two additional motivations have to be mentioned. The detection and measurement of both ^7Be and p-e-p lines would:

1) be a clear signature of the basic nuclear fusion processes inside the Sun (and the main sequence stars)

2) allow a precise temperature determination of the core of the Sun. In fact the production of ^8B neutrinos is impossible without the prior production of ^7Be. The ^8B neutrinos arise from proton capture by ^7Be, while the ^7Be neutrinos arise from electron capture. The former process is a strong function of the central solar temperature because of the high Coulomb barrier, whereas the latter process is weakly dependent upon temperature (it depends mainly on the density). Within the framework of the Standard Solar Model a 20% measurement of the ratio of the two fluxes would give the central temperature to better than 2%.

3. DETECTION PRINCIPLE

The inverse β-decay reaction on ^{115}In has a very low threshold (119 keV) and a very high sensitivity to the low energy neutrinos produced in the Sun. The reaction is:

$$\nu_e + {}^{115}In \rightarrow {}^{115}Sn^* + e^- \qquad (3)$$

and the relevant energy levels of ^{115}In and ^{115}Sn are shown in fig. 3.1. Neutrino capture with electron emission takes ^{115}In (96% natural abundance) to the second excited state of ^{115}Sn. The unique signature for neutrino detection is a pulse from the electron, followed by, on average 3 μs later, time-coincident pulses: one, γ_1, of energy 116 keV, in part internally converted and spatially very close to the electron and the second, γ_2, of energy 497 keV. The **kinetic** energy of the electron is $E_e = E_\nu - 119$ keV, so a measurement of its energy gives the neutrino energy. The expected electron energy spectrum based on the Standard Solar Model is shown in fig. 3.2 plotted in bins 20 keV wide.

For a scintillator detector the events due to p-p neutrinos will be swamped by accidentals due to the indium β-decay. However, the ^7Be and p-e-p peaks are beyond the end point of the β-decay spectrum, and, as we will show later, are expected to stand up above the background in a detector of appropriate energy resolution.

The first attribute of the signature is a **prompt event** defined as an isolated pulse of 743 keV (1323 keV for p-e-p neutrinos) within the energy resolution and contained in one "logical cell" *), the electron-cell.

---

*) A more precise definition of the logical cell, which is determined by timing between the two PMT's, will be given below, when we discuss efficiencies and backgrounds (sections 4 and 5).

The second attribute of the signature is a **delayed event** which is a delayed (within about 10 μs) energy release of 613 keV (the sum of the energies of γ_1, and γ_2) spatially close to the first event. The third attribute of the signature is related to the topology of the interactions of γ_1 and γ_2 and results in space and fast-time coincidences among the Compton and photo-electrons produced by γ_1 and γ_2 in two or more neighboring cells. In fact γ_1 will deposit its energy mainly in the electron-cell, while γ_2 will deposit energy in the electron cell and in the eight "logical cells" surrounding the electron-cell (see fig. 3.3). These three attributes of the overall signature have been extensively studied with Monte Carlo calculations as a function of the resolution in energy , space, and time (see sections 4 and 5).

Even so, at some level (which we have estimated) random coincidences in space and time of the indium β-decays plus stray γ-rays from natural radioactivity and residual cosmic ray interactions can mimic the solar neutrino events. This problem is discussed in detail in section 5.

In addition we can invoke the fourth attribute of the signature, namely that the solar neutrino events exhibit a time correlation between the prompt and delayed events due to the 3.3 μs half-life of $^{115}Sn^*$, whereas the background is time-uncorrelated. Moreover, this means that the experiment can measure its own background very precisely. There are some possible time-correlated backgrounds, for example the $^{212}Bi \rightarrow {}^{212}Po \rightarrow {}^{208}Pb$ and $^{214}Bi \rightarrow {}^{214}Po \rightarrow {}^{210}Pb$ decays, but these are negligible as will be shown in section 5.

Concerning the p-e-p neutrinos, we remark that there is no known state of energy between 613 keV and 1500 keV [a] with the appropriate spin-parity assignment for neutrino capture [3,1]. Therefore the signature of the delayed event remains the same for the p-e-p neutrinos as for ^7Be.

The expected interaction rates for the ^7Be and p-e-p neutrinos are respectively 0.5 and 0.04 / day for a detector containing 10 tons of indium. The actual event rates using estimated efficiencies will be discussed in section 4.

4. EFFICIENCY AND EVENT RATES

In the experiment we are considering, the **kinetic** energies of the electrons and γ's which need to be detected are the following:

$$E_{e^-} = 862 - 119 = 743 \text{ keV for } ^7Be \text{ line}$$

$$E_{e^-} = 1442 - 119 = 1323 \text{ keV for pep line}$$

$$E_\gamma = 116 + 497 = 613 \text{ keV in both cases}$$

The efficiency has been studied with a Monte Carlo program in which the electrons and γ's are propagated through indium foils of various thickness. Each thickness "t" corresponds to a particular design of a physical detector cell containing 10% of indium.

---

a) Should such a state exist, it would have a prompt γ decay the effect of which could however be suppressed by an anti-coincidence with the electron.

1) Indium loaded liquid scintillator corresponds to t=0, since the indium is uniformly distributed.
2) Thin indium plates associated with liquid or solid scintillator correspond to t=40 mg/cm^2.
3) Scintillating fibers coated with indium correspond to t=2.6 mg/cm^2. Here the fibers are approximated by a planar geometry. A simulation with the correct cylindrical geometry might give slightly different results and is being carried out.

4.1 Electron detection efficiency

In the case of indium loaded scintillator, the relevant parameter is the scintillator efficiency itself. When indium plates are used, the electron efficiency is affected by the absorption in the plates.

Since the prompt event requires a pulse of energy in the window 660 to 880 keV, as defined in the ^{7}Be trigger (see section 5), the energy resolution also influences the efficiency. A thickness of 40 mg/cm^2 should not be exceeded in order to achieve a reasonable efficiency. For the p-e-p detection (E_{e^-} = 1323 keV), the effect of the absorption in the plates is negligible.

Table 4.1 shows the electron detection efficiency for various indium plate thickness t and various energy resolution parameters $k=\sigma/\sqrt{E}$, when the required energy threshold is 660 keV.

Table 4.1

$k=\sigma/\sqrt{E}$	^{115}In plate thickness t (mg/cm^2)	Efficiency for $660<E_{e^-}<880$keV (%)
0	40	83
2.5	40	67
	2.6	80
	0	85
3.5	40	60
	2.6	75
	0	80
4	40	58
	2.6	74
	0	78

The effect of absorption and of the energy resolution is also illustrated in fig. 4.1 .

4.2 Gamma detection efficiency

The calculation of the γ-efficiency must take into account the cell size, the effect of the walls between cells, and the trigger configuration. As a first approach, we have estimated the efficiency on the basis of general considerations.

Clearly, the 116 keV γ_1 from the delayed event is confined lamost entirely to the cell in which the prompt event occurred (the "electron cell"). Considering that 35 cm is the typical distance to confine a 500 keV gamma ray (the γ_2 from the delayed event), we require for the delayed event simultaneous pulses in the "electron cell" and in a region around that cell, approximated by a 35 cm diameter sphere, with thresholds of 30 and 400 keV respectively. The calculated γ-efficiency is ≈ 60 % . When the threshold is raised to 50 keV, the efficiency drops to ≈ 45 %.

4.3 Event rates

The combined overall detection efficiency for electrons and γs is ≈ 30-40 % depending on the threshold chosen for the delayed event in the "electron cell" . For this matter, the cell with 40 mg/cm^2 indium plates is at a slight disadvantage with respect to the other types of cells (see Table 4.1).

The interaction rates of solar neutrinos on ^{115}In have been calculated in ref. [2,2] by using the solar neutrino fluxes and the indium capture cross sections. The expected interaction rate of ^{7}Be neutrinos is 0.5 per day in a detector containing 10 tons of indium. When the overall detection efficiency is taken into account, a safe estimate of the event rate is ≈ 1 per week.

As an example, if the ratio Signal/Background (S/B) is equal to 1, we need ≈60 events within three "50 keV" bins around 743 keV to establish a signal due to ^{7}Be neutrinos. This can be achieved in one year of data taking. The conditions to be met for reaching S/B>1 are described in the following section.

5. BACKGROUND

5.1 Generalities

As previously explained in section 3 and fig.3.3, the signal corresponding to a neutrino interaction in the detector will consist of one electron of 743 keV depositing its total energy in a single "logical cell" (cell No 1), except for a small proportion of bremsstrahlung which can escape the cell, followed, in less than 10μs, by two simultaneous γ rays of 116 and 497 keV. The first one is partly converted and deposits most of its energy in cell 1, while the second one will deposit its

energy mainly in cell No 1 and in the eight surrounding cells by multiple Compton scatterings. The dimensions of the "logical cell" will be important both for the efficiency and background requirements. Let us call M (in grams) the total mass of the cell and δ the proportion of indium. The dimensions are of the order of 12 to 15 cm in section and 30 cm in the longitudinal direction in order to form approximately a cube with 9 cells. The length of the logical cell is therefore n≈7 times smaller than the length of the physical cell (≈2 m) which will be built in a practical detector (see section 6).

Therefore the **trigger** will be defined by a two-fold coincidence between:

- a pulse of 743 keV in a single cell labelled cell No 1, the **prompt** event,
- at least two simultaneous pulses occurring respectively in cell No 1 and 2 to 9, with a total energy of 613 keV, the **delayed** event. This coincidence is expected in a time less than 10μs.

The types of background simulating this signature are the following:

1) for the **prompt** event occurring only in cell 1(and without any simultaneous pulse in cells 2 to 9)

- the tail of the indium β-decay spectrum which is smeared by the energy resolution.
- the pile-up of two β pulses in less than 10 ns in the same physical cell. (It is not possible to distinguish the positions of the two electrons emitted in less than 10 ns in the same physical cell).
- a β of ^{212}Bi or ^{214}Bi internal contamination of the detector (these two nuclides are grand daughters of ^{220}Rn and ^{222}Rn respectively)
- a Compton electron (or photoelectron) from an interaction of a background gamma coming from internal contamination or from external background.

2) for the **delayed** event :

- the tail of the In β spectrum associated with a bremsstrahlung photon in a neighboring cell.
- the pile-up of two β 's emitted in less than 10 ns in cells 1 and 2 to 9 respectively.
- an alpha of ^{214} Po ($t_{1/2}$=160 μs) followed simultaneously by a gamma of 800 keV from ^{210} Pb * (branching fraction =10^{-4}).
  There is no contribution of ^{212}Po which decays without an associated gamma.
- a multi Compton scattering of a gamma ray coming from inside or outside the detector.

It must be stressed that no other β-decay and no α-decay from possible additional contamination in the detector are taken into account both for the prompt and for the delayed event. The effect of such an additional contamination is examined in Appendix I.

5.2 β background

The β decay rate per gram of indium is $r_0 = 0.27$ Bq. The energy window used to detect the 743 keV electron produced by the neutrino interaction is defined between E_1 and $E_1 + \Delta E_1$, while the corresponding one for detecting the γ rays is between E_2 and $E_2 + \Delta E_2$. The values E_1, ΔE_1, E_2 and ΔE_2 have been preliminarily chosen as 660, 220, 400 and 400 keV respectively. Therefore the energy intervals are {660,880keV} for the electron and {400,800keV} for the γ rays. The different modes of contribution of the indium decay electron in these energy regions are listed in Table 5.1 where p_1,p_2 (p_3, p_4) are the proportions of the corresponding energy distributions included in the first (second) energy window. The values of p_2, p_3, p_4 are almost independent of the energy resolution $\sigma = k\sqrt{E}$ (see Fig 5.1 for p_2) with which the electrons are measured, and amount to .085, $2\ 10^{-7}$ and .55 respectively. The proportion p_1, which represents the tail of the β spectrum between E_1 and $E_1 + \Delta E_1$, is strongly dependent on σ. It has been calculated by folding the β spectrum obtained in ref. [5,1] with a Gaussian curve and is shown in figure 5.2 for a β spectrum end point $E_{max} = 494$ keV. Because there is an uncertainty of ≈3 % in the value of E_{max} [6,1], a calculation with $E_{max} = 482$ keV has also been made (not shown), and leads to values of p_1 which are 1.5 to 3 times lower, depending on σ. These curves are valid for an homogeneous detector. The corresponding p_1 and p_2 distributions, including absorption effects, have been obtained by a Monte-Carlo simulation and are also shown on Figs. 5.1 and 5.2.

Table 5.1

Definitions	Expressions	Comments
Prompt event		
β - tail	$b_{11} = r_0 \cdot M \cdot \delta \cdot p_1$	
β - pile up (same cell)	$b_{12} = n\,(r_0 \cdot M \cdot \delta)^2\, p_2 \cdot 2 \cdot 10^{-8}$	in the same physical cell
Delayed event		
β – bremsstrahlung in 2 diff. cells	$b_{21} = r_0 \cdot M \cdot \delta \cdot p_3$	only 1 surrounding cell
β – pile up 2 β *in 2 diff. cells*	$b_{22} = 8\,(r_0 \cdot M \cdot \delta)^2\, p_4 \cdot 2 \cdot 10^{-8}$	8 surrounding cells

With the expressions of table 5.1, the rate C_β per "logical cell" and per sec of random coincidences in 10 μs between the prompt and delayed event is :

$$C_\beta = 10^{-5} (b_{11} + b_{12}) (b_{21} + b_{22})$$
$$= 10^{-5} (r_0 M \delta)^2 (p_1 + n r_0 M \delta \cdot 2\ 10^{-8} p_2) (p_3 + 16\ 10^{-8} r_0 M \delta \cdot p_4)$$

The term b_{22} is much larger than b_{21} which can be neglected . Except for small values of k (≤ 2.5), b_{12} is much smaller than b_{11}.

Using the values calculated for p_2, p_3, p_4 and taking $n = 7$ (2.1 meter length for a physical cell) one gets:

$$C_\beta = 0.17\ 10^{-19} M^3 \delta^3 (10^6 p_1 + 3\ 10^{-3} M \delta)$$

The expected number of neutrino events per "logical cell" and per sec, S, is, assuming a total efficiency of 50% :

$$S = 0.29\ 10^{-12} M \delta$$

The ratio

$$S / C_\beta = 1.7\ 10^7 / (M \delta)^2 (10^6 p_1 + 10^{-3} M \delta)$$

is plotted in figure 5.3 as a function of k for a"logical cell" of (12x12x30)cm^3 (M=4840 g, ρ=1.12) with $\delta = 0.1$ and for the three types of detectors considered. For a detector made of indium plates or scintillating fibers, the indium absorption of the electrons is slightly larger for β 's from Indium decay than for electrons from neutrino interactions, resulting in better signal / background ratios.

5.3 γ background

With the trigger logic previously described, the delayed pulse is due to simultaneous events in 2 (or more) neighboring cells including cell 1. The main source of background is due to the multi-Compton scattering of γ 's. However , the ^{214}Po $\alpha\gamma$ decays may also contribute. An evaluation of this effect shows that it is negligible compared to the multi-Compton contribution (see Appendix II).

Therefore the prompt and delayed event rates, per "logical cell" and per sec, g_1 and g_2 are respectively :

$$g_1 = G \cdot M \cdot \Delta E_1$$
$$g_2 = 2\ a \cdot \Delta E_2 \cdot G \cdot M$$

where G is the background rate per (keV.g.s), at an energy around 600 keV; a is the proportion of multi-Compton scattering between cell 1 and one (or more) neighboring cell (or vice-versa, explaining the factor 2) deposing an overall energy between E_2 and $E_2 + \Delta E_2$ in the nine cells. The parameter a has been evaluated to be 0.3.

So, the random coincidence rate C_γ between the prompt and delayed events is :

$$C_\nu = 10^{-5} g_1 g_2 = 2\,10^{-5}\, a\, \Delta E_1 \Delta E_2\, G^2 M^2 = 0.53\, G^2 M^2$$

and the ratio $S / C\gamma$ can be expressed as:

$$\frac{S}{C_\gamma} = \frac{0.29\,10^{-12} M \delta}{0.53\, G^2 M^2} = \frac{0.55\,10^{-12}\delta}{0.53\, G^2 M} = \frac{2.1\,10^{-17}}{G^2}$$

This ratio is plotted as a function of G in fig. 5.4. for the three types of detectors considered.

The rate G of the γ background may be evaluated from the data obtained by the double β experiments performed with Ge crystals in very low background environments. Table 5.2 summarizes the results obtained in various experiments generally done in underground laboratories and with a very good shielding .

Table 5.2

EXPERIMENT		SITE	SHIELDING	(COUNTS / g.sec. keV) x 10^9 (around 500 keV)
Bordeaux 88	[5,2]	Fréjus	15cm Pb + 5cm Cu	6
Bordeaux 8ó	[5,2]	Fréjus	15cm Pb + 5cm Cu +plastic	5
Gif 89	[5,3]	Fréjus	15-20cm Pb + 5cm Cu +2cm Al	15
CALTEC-SIN--Neufchatel	[5,4]	Gotthard	18cm Pb + 15cm Cu	8
S.Barbara-Berkeley	[5,5]	California Dam	20cm Pb +active shield	3

These experiments are shielded with 15 to 20 cm of lead and 5 to 15cm of copper. A reasonable low limit of G is about $4\,10^{-9}$ counts/keV.g.s. in the region of 600 keV. Now we have to extrapolate this value to a large detector of the order of $(5m)^3$. The main background in germanium experiments is probably not due to internal contamination. If it was so, it would correspond to a contamination of the order of 10^{-10} g of ^{238}U per g of detector (if one assumes the Uranium chain to be in equilibrium) whereas in liquid scintillator, a level below 10^{-11} g of ^{238}U per g of detector has been measured [5,6]. If therefore this background comes mainly from a contamination outside the detector (hence only gammas), then it could be extrapolated according to the area of the detector or the inside area of the shielding. For a 500 g Ge detector, the ratio area / mass is about 0.24 cm^2/g , while for a $(5m)^3$ scintillator it is 0.01, and the self shielding is very important. We will in this hypothesis decrease the intensity G by a factor of 20 .

Therefore the gamma background in a large detector of the same purity as a Ge detector would probably range from $G = 4\ 10^{-9}$ to $G = 2\ 10^{-10}$ depending on which extrapolation is used (according to the mass or to the area). This would lead (fig. 5.4) to ratios S/C_γ ranging between 1 and about 200.

Recently, background measurements were made in the underground Fréjus laboratory with a liquid scintillator as well as with scintillating fibers (see Appendix III). These detectors which are realistic candidates for the final detector were placed inside a shielding made of lead and copper. The results obtained up to now indicate that the total background must be decreased by ≈ 2 orders of magnitude in order to satisfy the feasibility conditions for this experiment.

5.4 Signal / Background

The total background is obtained by adding, in the prompt and delayed events, the β and γ contributions :

$$B = 10^{-5} (b_{11} + b_{12} + g_1) (b_{21} + b_{22} + g_2)$$

Neglecting b_{21} and for δ=0.1 and M = 4840 g , one obtains :

$$B = 10^{-5} (130.7 \{p_1 + 18.2\ 10^{-6} p_2\} + 1.06\ 10^{6} G) (2.7\ 10^{-3} p_4 + 1.16\ 10^{6} G)$$

The ratio S/B has been calculated for several values of G between 10^{-10} and 10^{-8} counts/keV.g.sec and for the values of $k = \sigma/\sqrt{E}$ between 2.5 and 5.

Figure 5.5 shows, as a function of G and k , the curves for which the value S/B is 0.1, 1 and 10 respectively for an homogeneous detector, an indium plate detector (40mg/cm^2) and a fiber detector simulated by a plate detector with 2.6 mg/cm^2 of indium sheets separated by 1 mm plastic scintillator. The variation of S/B is extremely sensitive to the resolution which must be smaller than 12% at 743 keV in order to reach a signal larger than the background even in the case of an optimistic extrapolation of the γ background.

The p-e-p ν's of 1442 keV produce, by inverse β decay on the $7/2^+$ excited state of ^{115}Sn , an electron of 1323 keV. Therefore the signature is identical to the one for ^{7}Be ν's except that the prompt pulse consists of an electron of 1323 keV. At this energy one can neglect the tail of the indium β ray and only the γ background remains. From double β decay experiments, this background is about 5 times smaller than around 700 keV. However, taking the calculation of Bahcall [2,2],[2,10], the ν interactions are 14.3 times smaller with the p-e-p ν's than with the ^{7}Be ones. Therefore the S/B ratio will be about 3 times smaller than the S / C_γ ratio shown in fig. 5.4. (Nevertheless when comparing S/B ratios one must realize that the β-tail only contributes to the background in the case of ^{7}Be neutrinos). This means that a ratio $S / B > 1$ can be reached for $G < 2\ 10^{-9}$/keV.g.sec at 700 keV.

6. POSSIBLE DETECTORS AND THEIR PERFORMANCE

A solar neutrino interaction rate of 0.5 per day from ^{7}Be requests a detector containing 10 tons of indium. The detector would consist of ≈ 100 tons of scintillator with 10% of indium inserted. The scintillator must be optically divided into a large number of **physical cells** of adequate dimensions (e.g. 12 cm x 12 cm x 200 cm). This is because the counting rate per cell must remain reasonable in order to maximize the value of S/B, as explained in section 5. The detector would therefore consist of ≈ 3000 physical cells and ≈ 6000 photomultipliers (PMT).

The **logical cell** (e.g. 12 cm x 12 cm x 30 cm) can then be defined by using timing between the two PMT's located at both ends of a physical cell.

Three possible designs of a physical cell have been considered: 1) Indium loaded liquid scintillator, 2) Thin indium sheets associated with liquid or solid scintillator, 3) Scintillating fibers coated with indium (see Fig. 6.1).

6.1 Indium loaded liquid scintillator

Several attempts have been made to produce liquid scintillator loaded with an adequate amount (5-10%) of indium and with acceptable performances. Until recently, the short attenuation length and the stability over a long period of time have been the unsolved problems for this product.

Measurements of the energy resolution have been made with indium loaded liquid scintillator. In early measurements [5,1], a liquid scintillator loaded with 51 g of indium per liter (≈ 5% loading) was used. The liquid was contained in a 10 cm long cylinder, 12 cm in diameter. The measured energy resolution $\sigma(E)/E$ was 8%. Because the cell was only 10 cm long, the effect of light attenuation cannot be seen in this measurement.

Another measurement was made with indium loaded scintillator contained in a 1 meter long cylindrical cell of 6 cm diameter [6,1]. Using the backward scattered gamma ray of a ^{137}Cs source as a tag, the associated ≈ monoenergetic electron (477 keV) is measured.

At the September, 1989 meeting at Collège de France, new results were reported. NE Technology Ltd. [6,2] delivered a compound based on pseudocumene containing 5 % of indium. Measurements in a 1 m long cell show significant improvement in the energy resolution.

Our colleagues from Japan [6,3] have obtained new results with a liquid scintillator based on xylene containing 7 % of indium. The energy resolution obtained in a 1 m long cell is similar to the NET result.

Table 6.1 shows the results obtained with indium loaded liquid scintillator. The quoted energy resolutions are for 743 keV, assuming that $\sigma = k\sqrt{E}$

$7/2^{+}$ 613

Table 6.1

Energy resolution of indium loaded liquid scintillator measured in a 1 m long cell.

Reference	[5,1]	--------	[6,1]	----------	[6,2]	[6,3]
indium loading	5%	0	5%	10%	5%	7%
σ(E)/E (%) at 743 keV	"8" 10cm cell	8	18	30	≈13	≈13

It is clear that the latest measurements [6,2], [6,3] show significant improvement over previous results. However, the indium loading is still limited to 5-7 % and the cell length to 1 meter.

6.2 Thin Indium sheets associated with scintillator

A set up consisting of a sandwich of thin indium sheets and scintillator plates was tested by R. Raghavan as early as 1978 [6,4]. The set up was made of a 7-layer sandwich of 7 mg/cm^2 thick indium sheets and 1.6 mm thick plastic scintillator plates, 5 cm wide and 1 meter long and was a preliminary design for a detector aimed at measuring the low energy p-p neutrinos. This arrangement corresponds to ≈ 6% indium loading. The resolution was σ(E)/E =11% at 743 keV.

The performance of such a cell has been measured with a similar set up [6,5]. A one meter long NE102 plastic scintillator sheet (60 mm wide, 5 mm thick) was equipped with a PMT at each end.

Electrons from a ^{207}Bi conversion source (E_e = 870 and 480 keV) were used in both tests. The measured energy resolution are shown in Table 6.2 and compared with the case of liquid scintillator (§6.1).

Table 6.2

Measured energy resolution at 743 keV in thin plastic scintillator plates compared to pure liquid scintillator.

Scintillator type	liquid - ref.[6,1]	plastic - ref.[6,4]	plastic - ref.[6,5]
geometry	Cylinder: ϕ=6cm, l=100cm	0.16cm x 5cm x 100cm	0.5cm x 6cm x 100cm
Number of scintillator sheets in stack		7	1
σ(E)/E (%) at 743 keV	8	11	13

It should be remarked that these measured resolutions do not only reflect the intrinsic performance of scintillators but also the particular features of the experimental arrangements.

A possible scheme for a cell would consist of a box containing 24 indium metal sheets, 12 cm wide, 200 cm long and 40 mg/cm^2 thick, supported by thin acrylic frames and adequate supports to provide the necessary rigidity. The space between the indium sheets is 5 mm and is filled by mineral oil-based liquid scintillator. At each end of the cell, a window is provided for the PMT's. This cell would have an indium loading of 8%. Such a cell is under construction and will be tested soon [6,6].

6.3 Plastic scintillating fibers

The use of scintillating fibers coated with indium was suggested several years ago [6,7].

A cell would consist of a bundle of 1-mm diameter scintillating fibers, each fiber being coated with 3.6 μm of indium metal. This coating gives an indium loading of 10% by weight. Bundles of fibers 12 cm x 12 cm in area and 200 cm in length are optically coupled to PMT's.

In order to measure the energy resolution, fibers developed at Saclay for the UA2 experiment were used to build a 2 meter long prototype cell of reduced cross section 2 cm x 3 cm. The stack contained 600 fibers. There was no indium coating, but it is not expected that 3.6 μm of indium will degrade the energy of the e^- in a significant way. The cell was viewed by a PMT at each end. The zero degree Compton electrons of ^{54}Mn and ^{137}Cs sources (electron energy: 644 and 477 keV, respectively) were used. The energy resolution was found to be $\sigma(E)/E = 17$ % at 743 keV [6,8]. The experimental procedure has been checked by measuring the energy resolution in a small NE110 plastic scintillator which gave a resolution of 12 % .

The result obtained with these fibers agrees with expectations from the performance of the UA2 fibers [6,9],[6,10]. Fibers manufactured in Japan by KYOWA have also been measured for their light output and attenuation length; the performances relevant to this study are very close to those of the Saclay fibers [6,10].

To compare these performances of fibers to the indium-loaded liquid scintillator we have used the known attenuation length to calculate the energy resolution for a 1 m long fiber detector. We find $\sigma/E \approx 14$ % at 743 keV in agreement with preliminary measurements.

The measurement of the energy resolution function in fibers has shown that there is a high-end tail compared to a normal distribution. Therefore it is very likely that Monte Carlo calculations using normally distributed resolution functions underestimate the background due to the indium β-tail by about a factor of 2.

6.4 Comparison of designs

In all three designs there is potential for improvement in order to achieve the desired energy resolution of $\sigma(E) = 2.7\sqrt{E}$, i.e. $\sigma(E)/E = 10\%$ at 743 keV in a 2 m long cell loaded with 10 % of indium.

a) Recent measurements with indium loaded liquid scintillator [6,2], [6,3] give an energy resolution $\sigma(E)/E \approx 13$ % at 743 keV. It must be noted, however, that the indium loading was limited to 5-7 % and the length of the cell was only 1 m. On the other hand, the possibility of using Pulse Shape Discrimination (PSD) to identify α and β particles in liquid scintillator is an asset for background identification [6,11].

b) It was shown in section 5.2 that, compared to the case of indium loaded liquid scintillator, the insertion of indium in the form of thin sheets (not exceeding ≈40mg/cm2) will not degrade the performance of the cell from the physics point of view. On one hand, the signal is broadened because the electron loses energy in the indium sheets, but on the other hand, the energy of the indium β background is even more degraded so that the contamination of the signal is decreased.

A cell with thin indium plates imbedded in plastic or liquid scintillator appears to have the best energy resolution because the scintillator remains pure. The thickness of the indium sheets must be limited to ≈ 40 mg/cm^2 to avoid too much energy loss in indium. In order to get ≈10 % indium loading, the scintillator sheets must be thin (≈ 5 mm); the main difficulties come therefore from the light propagation and reflection in thin and long layers of liquid scintillator. A measurement of the energy resolution in such a cell is not yet available.

c) With scintillating fibers coated with indium, there is the possibility of "diluting" the indium inside the detector without disturbing the scintillation medium. For a 10% loading, only 3.6 μm of indium around fibers 1mm in diameter and 2 meter in length are needed. The measured energy resolution, $\sigma(E)/E = 17$ % at 743 keV, was obtained in a 2 m long cell and has its limitation in the light output and propagation in fibers. It is likely that improvement in scintillating fiber performances will be made, since there is much development work in progress. For this application, the light output and light collection must be improved, and the coating of indium around the fibers must be studied.

$$\frac{\sigma}{E\,(keV)}\,(\%) \quad \text{at} \quad 743\,keV$$

7. FUTURE TESTS AND DEVELOPMENTS

In order to get a definitive answer to the feasibility of a real time ^{115}In experiment we have to demonstrate the possibility to limit the γ background at a level of a few 10^{-9} count/keV· g· s , and to improve the energy resolution of our detector down to σ/E values in the range of 10 to 12% at 700 keV(see section 5.4).

For the study of the internal gamma rays background, in the different types of detector cells, measurements inside an appropriate shielding in a location protected from cosmic rays, such as the Fréjus laboratory, will be necessary. In addition, to avoid background from the PMT's, light guides must be used to keep the tubes away from the scintillating material.
We propose to build various cell prototypes and to perform these background measurements.

In order to do so, we intend to use the existing lead-copper shielding in the Fréjus laboratory, possibly in association with a Germanium detector. We also are studying the possibility of using a pool of purified water of much larger size. This installation could in fact be useful as a test facility for detector prototypes of several low background experiments.

The second question is to evaluate the effort and time scale to sufficiently improve the energy resolution.

8. CONCLUSIONS

a) The present data on the solar neutrinos are very scanty. The experiments in preparation (GALLEX / SAGE) or in project (BOREX,SNO) will probably not be able to get alone the complete answer to the solar neutrino problem due to the complexity of the possible interpretation (MSW effect) involving the knowledge of the energy spectrum of the neutrino flux in a critical way.

b) Therefore the original idea (R.S. Raghavan, 1976) of using the inverse β–decay of ^{115}In to provide a unique delayed coincidence signature for the solar neutrinos is re-considered to detect the ^{7}Be and p-e-p lines. These are expected to stand up well above the continuum, in the intermediate region of the energy spectrum. In addition this type of measurement can measure its own background very precisely.

c) Preliminary investigations indicate that such an experiment is feasible provided that a sufficient energy resolution (σ/E in the range of 10 to 12%) and a low level background (of the order of a few Becquerels per ton) are achieved.

d) To study the background problem in a realistic way , we consider the possibility of installing a "swimming pool" of about 50 m^3 purified water in the Fréjus Laboratory as a facility which could be used by all experimenters preparing low background experiments.

e) In order to achieve the required energy resolution, a very qualified R&D effort is needed to improve the performance of scintillating fibers. The same is true for liquid scintillator

$$\frac{\sigma}{E\ (keV)}\ (\%) \quad \text{at} \quad 743\ keV$$

loaded with 10 % of indium. In both cases light output and attenuation length must be improved. Recent progress in this matter looks promising.

$$\frac{\sigma}{E\,(keV)}\,(\%) \quad \text{at} \quad 743\ keV$$

CONTRIBUTION TO THE BACKGROUND BY A ^{210}Pb CONTAMINATION

^{210}Pb	$T_{1/2}$ = 22 years	β^- 17 keV (85%) γ 46 keV (≈ 5%)
$^{210}Bi^*$	$T_{1/2}$ = 5 days	β^- 1.17 MeV (≈100%)
^{210}Po	$T_{1/2}$ = 138 days	α 5.3 MeV → ^{206}Pb (≈100%) α 4.5 MeV → $^{206}Pb^*$ → (γ 800keV) ^{206}Pb (B.R. 1.2 10^{-5})

1. Measurement in the Fréjus Laboratory (see Appendix III)

In the liquid scintillator of the Bugey cell measured in the Fréjus laboratory, 0.14 Bq of ^{210}Po is found for 6000 g of scintillator. This corresponds to 8 10^{-18} g of ^{210}Pb / g of detector. If this contamination is due to an admixture of radon during the manufacturing process of the scintillator, it would correspond to the absorption in 6 liters of scintillator of the radon contained in ≈18 m^3 of air in a few days (assuming ≈ 20 Bq of radon per m^3 of air).

2. Qualitative effect

In the background calculated with the trigger defined in this Progress Report this contamination contributes to the background in two ways:

a) Purely random coincidences due to the β of ^{210}Bi and α of ^{210}Po (unless they can be identified by the PSD technique).

b) Real coincidences between an α and a γ in the delayed pulse (B.R. = 1.2 10^{-5}) in random coincidence with a β or α in the prompt pulse.

3. Quantitative calculation

a) Taking the formula of section 5.4 which evaluates the background **without** the ^{210}Pb contamination we get:

$$B = 10^{-5} P D$$

where the "prompt" intensity for a 4840 g cell is:

$$P = 130 (p_1 + 18\ 10^{-6} p_2) + 10^6 G$$

and the "delayed" intensity for the same cell:

$$D = 2.7\ 10^{-3} p_4 + 1.2\ 10^6 G$$

This gives the results presented in the first line of table I where the following values of the parameters are assumed:

$p_1 = 5\ 10^{-5}$ corresponding to a homogeneous detector with $\sigma / E = 12\%$ (Fig. 5.2), $p_2 = 0.085$,

$p_4 = 0.55$ (see section 5.2), and $G = 5\ 10^{-9}$.

b) The two contributions of ^{210}Pb are calculated assuming a contamination of 0.1 Bq in a 4840 g cell. We have assumed that 30 % of the ^{210}Bi β's fall into the prompt energy window (660-880 keV) and 50% of the α do the same.The fraction of events falling into the "delayed" energy window (400-800 keV) was taken as 50% for β's and 100% for α's.

Table I

counts / cell

	P	D	B
Background without ^{210}Pb contamination	**$12\ 10^{-3}$**	**$7.4\ 10^{-3}$**	**$9\ 10^{-10}$**
Purely random coinc. from ^{210}Pb	**$8\ 10^{-2}$**	$7\ 10^{-10}$	$6\ 10^{-16}$
^{210}Pb α–γ coinc. from ^{210}Po	$8\ 10^{-2}$	$7\ 10^{-7}$	$6\ 10^{-13}$
Background + ^{210}Pb	**$92\ 10^{-3}$**	**$7.4\ 10^{-3}$**	**$7\ 10^{-9}$**

4. Conclusion

The effect of a contamination of ^{210}Pb is to increase only the rate of the prompt pulse. With the contamination measured in the Bugey scintillator cell, corresponding to $8\ 10^{-18}$ g of ^{210}Pb per g of detector, this would increase by roughly one order of magnitude the rate of the prompt pulse due to the tail of the indium β spectrum above 660 keV as calculated with a Gaussian energy resolution (and for $\sigma/E = 12\%$).

Therefore the contamination of ^{210}Pb must be kept below a few $\mathbf{10^{-19}}$ g / g of detector to be acceptable for a solar neutrino experiment. This means that extreme care must be taken in the manufacturing process of the scintillator and of the rest of the detector to avoid the radon induced contamination.

APPENDIX II

Contribution of the ^{214}Bi internal contamination to the background per "logical" cell.

We present here an estimation of the background contribution, due to the possible presence of ^{214}Bi and ^{212}Bi inside the detector, to both **prompt** and **delayed** events (real coincidences) as discussed in section 5.

The relevant decay chains are :

$$^{214}Bi \rightarrow \beta^- + {}^{214}Po \quad (t_{1/2}=160\,\mu s)$$
$$\rightarrow \alpha\,(7.8\ MeV) + {}^{210}Pb^*$$
$$\rightarrow \gamma\,(0.8\ MeV) + {}^{210}Pb$$

and the similar chain for ^{212}Bi.

The corresponding background contributions are given, for a "logical cell" of dimensions 12cm x 12cm x 30cm and mass M(grams), in the following table :

Configuration	particles involved	Energy window	cell Nb	background contribution counts / sec
prompt event	β^-	660 to 880 keV	1	$k_1\, k_2$ Bi M
delayed event	α, γ	400 to 800 keV	1 and 2 to 9	$0.005\ 10^{-4}\ k_3$ Bi M
real coincidences in 10μs	β^- α,γ			$5\ 10^{-6}\ k_1\, k_2\, k_3$ Bi M $3\ 10^{-8}$ Bi M

where :

- Bi is the ^{214}Bi decay rate per g of detector and per sec
- the factors 0.005 and 10^{-4} represent the proportion of ^{214}Po decays in 10μs and the branching fraction to ^{210}Pb*, respectively
- k_1 is the probability for a β^- of ^{214}Bi to be in the "prompt event" window (20%)
- k_2 is the probability for the ^{214}Bi γ's not to be detected in cells 2 to 9 (30%)
- k_3 is the probability for the 7.8 MeV α plus the 0.8 MeV γ to be in the "delayed event" window (10%)

The following remarks are in order :

a) concerning the ^{212}Bi , it cannot contribute to the "delayed event" (and, as a consequence, to the real coincidences) background, because the ^{212}Po decays without associated γ.

b) the effect of the ^{214}Bi (β α,γ) decays is negligible compared to the signal : in fact, for a contamination of 10^{-10} g of ^{238}U / g of scintillator (in a ^{238}U chain in equilibrium) it amounts to less than 10^{-3} of the neutrino signal.

BACKGROUND MEASUREMENTS IN THE FREJUS LABORATORY

1. Detectors used:

D1: Lithium loaded liquid scintillator (Pseudocumene + 0.15 % lithium)

Total weight=6000 g

D2: Scintillating fibers (UA2 type)

Total weight=2400 g

PMTs are "low radioactivity" in both cases (^{40}K activity: 9 Bq /PMT)

2. Shielding:

S1: 15 cm lead + 0.5 cm copper

S2: 10 cm lead + 5 cm copper

3. Results:

	Energy Intervals	Units	D1	D2
S1	> 200 keV	counts/s	2.2	1.0
	> 200 keV	counts/g.s	$0.3\ 10^{-3}$	$0.4\ 10^{-3}$
	(400-800 keV)	counts/g.s.keV	$2\ 10^{-7}$	$5\ 10^{-7}$
S2	> 200 keV	counts/s	1.7	
	(400-800 keV)	counts/g.s.keV	$2.4\ 10^{-7}$	

4. Comments:

The internal background due to ^{210}Pb and ^{214}Bi has been measured with D1(*), using the Pulse Shape Discrimination technique (PSD) to identify α particles:

^{210}Po: 0.14 / s corresponding to $8\ 10^{-18}$ g of ^{210}Pb / g of detector (see Appendix I).

^{214}Bi: $0.9\ 10^{-3}$ / s corresponding to 10^{-11} g of ^{238}U / g of detector (if it is in equilibrium with Uranium) - (see Appendix II)

(*) Bugey Collaboration, to be published in Nucl. Instr. and Meth.

At present, the total background is two orders of magnitude larger than the upper limit acceptable for the solar neutrino experiment.

The contributions to the background above 200 keV have been evaluated:

≈ 15 % from the PMT's (^{40}K)

≈ 15 % from the internal contamination dominated by ^{210}Pb and its daughters.

≈ 70 % undefined, possibly from outside the detector.

The contribution of radon gas located inside the lead shielding was found to be negligible.

5. Neutron background:

The neutron background (energy above ≈ 2 MeV) was measured with detector D1. The result is 2 neutrons / day in the detector. With the known neutron efficiency of the detector (1%), this corresponds to 10^{-6} n/s.cm^2 above 2 MeV.

References

[1,1] R.S. Raghavan, Phys. Rev. Lett. 37 (1976) 259

[1,2] - N.E. Booth, G.L. Salmon, and D.A. Hukin, (1985) in *Solar neutrinos and Neutrino Astronomy,* AIP Conference Proceedings No. 126, edited by M.L. Cherry, W.A. Fowler, and K. Lande (AIP, New York), p. 216.

- N.E. Booth, Appl. Phys. Lett., 50, (1987) 293

[1,3] A. de Bellefon, P. Espigat, and G. Waysand, (1985) in *Solar neutrinos and Neutrino Astronomy,* AIP Conference Proceedings No. 126, edited by M.L. Cherry, W.A. Fowler, and K. Lande (AIP, New York), p. 227.

[2,1] R. Davis, Jr., in Proc. of *"Neutrino '88"*, Tufts University, June, 1988.

[2,2] J.N. Bahcall and R.K. Ulrich, Rev. Mod. Phys. Vol. 60, No 2 (1988) 297

[2,3] S. P. Mikheyev and A.Yu. Smirnov, Nuovo Cim. 9C, 17 (1986); L. Wolfenstein, Phys. Rev. D 20, 2634 (1979).

[2,4] S. Turck-Chieze et al., Astrophys. J. 335 (1988) 415

[2,5] T. Kirsten, 1986, in *" '86 Massive neutrinos in astrophysics and in Particle Physics"*, edited by O. Fackler and J. Tran Than Van, (Editions Frontières), p. 119.

[2,6] I. R. Barabanov, et al., 1985, in *"Solar Neutrinos and Neutrino Astronomy,"* ed. M. L. Cherry, W. A.Fowler, and K. Lande (AIP Conf. Proc. N° 126, New York), p. 175.

[2,7] K. S. Hirata et al. Phys. Rev. Lett. 63 N°1, (1989) 16

[2,8] R. S. Raghavan et al., Phys. Rev. Lett. 57 , (1986) 1801

[2,9] G. Aardsma, et al., Phys. Lett. 194 N° 2, (1987) 321.

[2,10] J.N. Bahcall and R.M. May, Astrophys. J. 155 (1969) 501

[3,1] Tables of Isotopes. Edited by C.M. Lederer and V.S. Shirley (7th Edition), 1978.
J. Blachot and G. Margnier, Nuclear Data Sheets 52 (4), (1987), 565.

[5,1] L. Pfeiffer et al., Phys. Rev. Lett. 41 (1978) 63 , and Phys. Rev. C, 19 (1979) 1035.

[5,2] Ph. Hubert et al., CEN Bordeaux-Gradignan, private communication.

[5,3] J.L. Reyss, Centre des Faibles Radioactivités-CNRS/CEA, 91191 Gif-sur-Yvette, private communication.

[5,4] P. Fisher et al. Phys. Lett. B218, (1989) 257.

[5,5] D.O. Caldwell et al., Phys. Rev. Lett. 59, (1987) 419.

[6,1] A.G.D. Payne and N.E. Booth, Tests of some prototype Indium-loaded scintillators for solar neutrino detection. Oxford University, Nuclear Physics Lab. Report, ref. 82/88.

[6,2] NE Technology Ltd., Sighthill, Edinburgh EH11 4BY Scotland. Results reported by G.L. Salmon (Oxford Univ.) at Collège de France in September 1989.

[6,3] Y. Suzuki et al., "Development of an Indium-Loaded Liquid Scintillator with Long Attenuation Length for ^{7}Be and p-e-p Solar Neutrino Detection", presented at CdF in September 1989 and submitted to Nucl. Instr. and Meth.

[6,4] R.S. Raghavan, 1978. (see report of March, 1989 at CdF)

[6,5] Results reported by N. Booth at the meeting at CdF in March, 1989.

[6,6] This cell is being built and tested at the University of Pennsylvania.

[6,7] R.S. Raghavan, in Proc. of "Neutrino '81" , Vol. 1, Maui, Hawaii, edited by R.J. Cence, E. Ma, A. Roberts

[6,8] Results reported by J. Ernwein (Saclay) at CdF, September, 1989.

[6,9] J. Alitti et al., Nucl. Instr. and Meth. A273 (1988) 135.

[6,10] M. Bourdinaud, DPhPE-Saclay, private communication.

[6,11] See the report by J.F. Cavaignac at CdF in September, 1989.

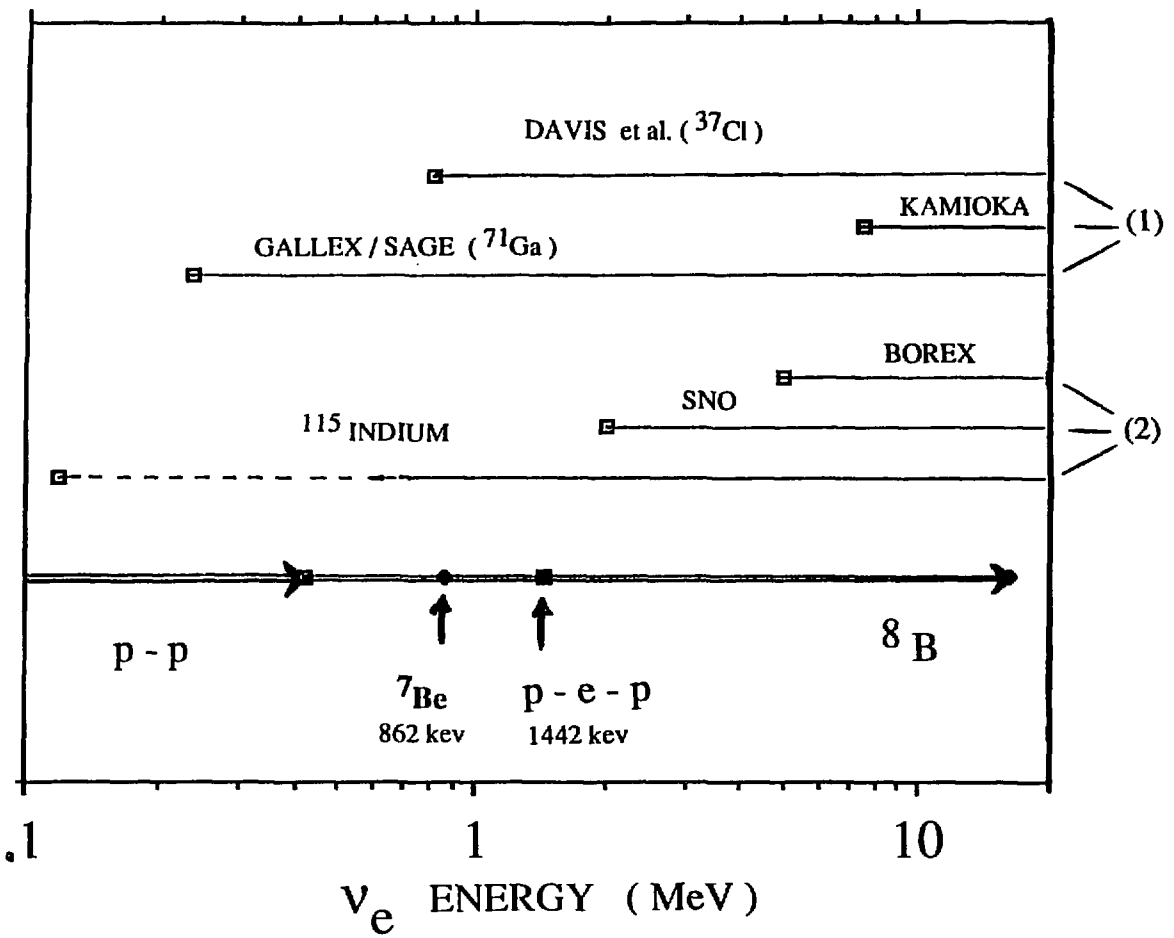

Fig. 2.1 The energy range accessible to the solar neutrino experiments in progress (1) and being planned (2) is shown together with the corresponding solar neutrino production mechanisms.

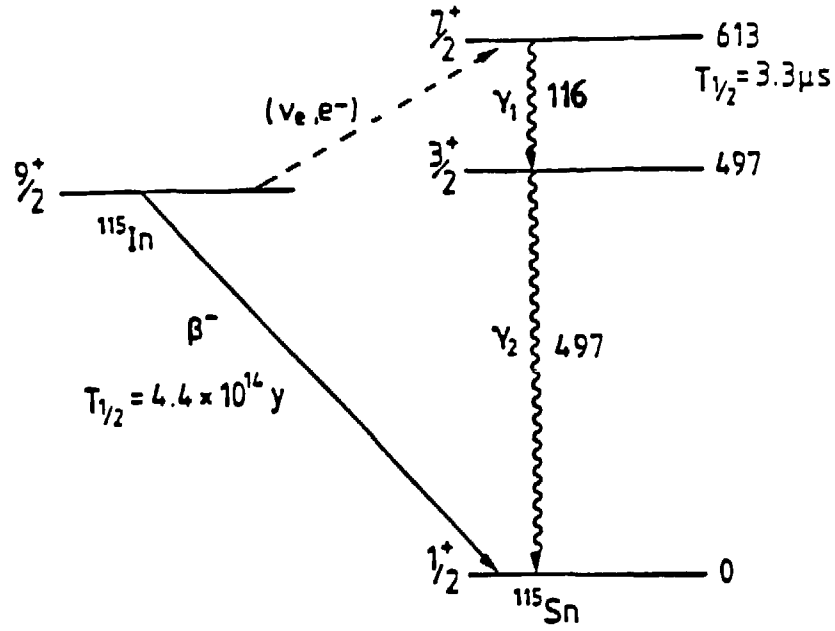

Fig. 3.1

Energy diagram of the ^{115}In neutrino capture reaction.

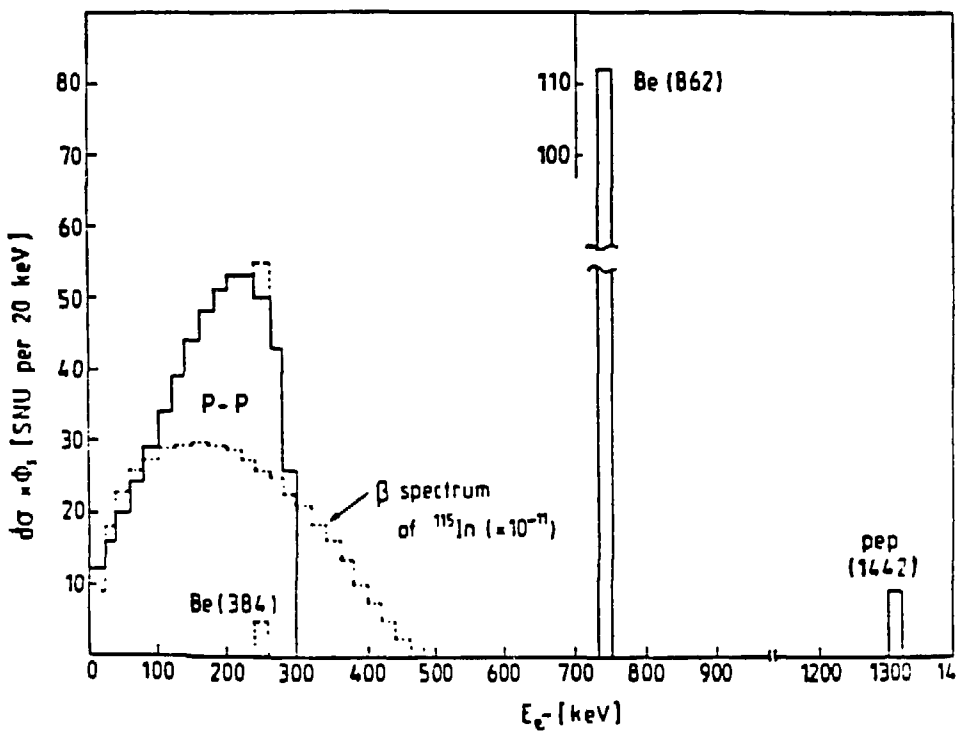

Fig. 3.2

Expected electron energy spectrum from an ^{115}In solar neutrino experiment, plotted in bins 20-keV wide. Also shown is the β-decay spectrum of ^{115}In converted to SNU and multiplied by 10^{-11}. The SNU (Solar Neutrino Unit) is the rate per second per 10^{36} ^{115}In atoms.

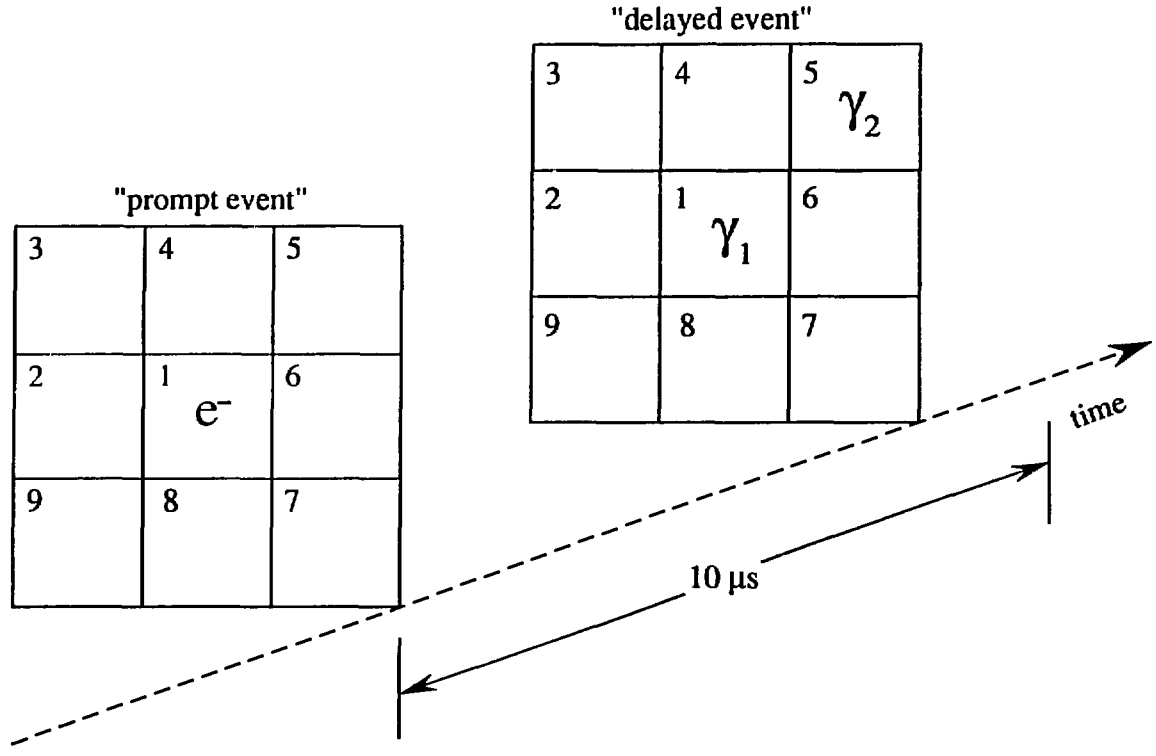

Space-time schematic representation of the inverse β-decay reaction :
$\nu_e(862\ keV) + {}^{115}In \rightarrow {}^{115}Sn^* + e^-(743\ keV)$
$\hookrightarrow \gamma_1(116\ keV) + \gamma_2(497\ keV)$

Fig. 3.3

The trigger is made of two components :

1) the **"prompt event"**: an isolated pulse due to the e^-, in an energy window around 743 keV (or 1323 keV for p-e-p neutrinos) and contained in a single logical cell labelled No 1.
2) a **"delayed event"**: an energy release of 400 to 800 keV, within 10µs, due to γ_1 and γ_2, in at least two neighboring cells including cell No 1.

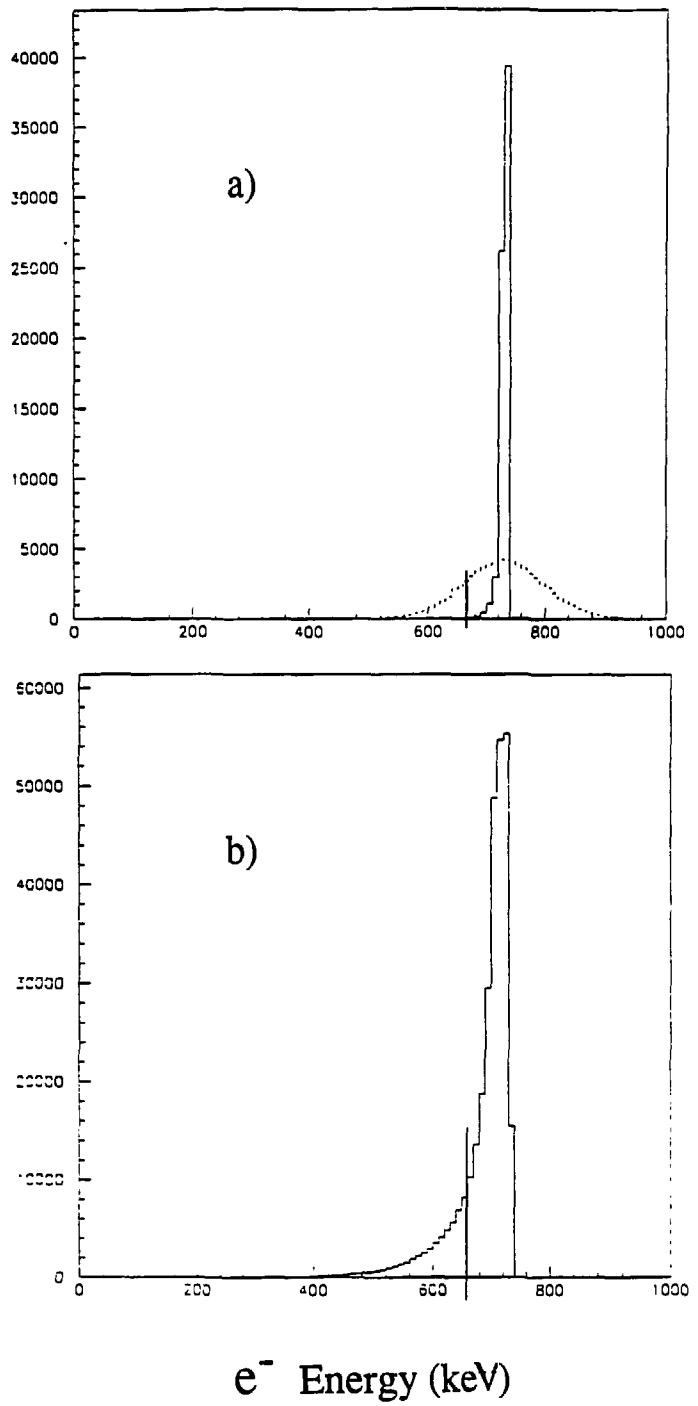

Fig. 4.1 a) Energy distribution of electrons emerging from the 2.6 mg/cm^2 indium plate where electrons of energy 743 keV are generated uniformly inside the plate. The dotted line represents the energy distribution folded with an energy resolution corresponding to $k=\sigma/\sqrt{E}=2.5$.
b) The same energy distribution is shown for an indium plate thickness of 40 mg/cm^2.

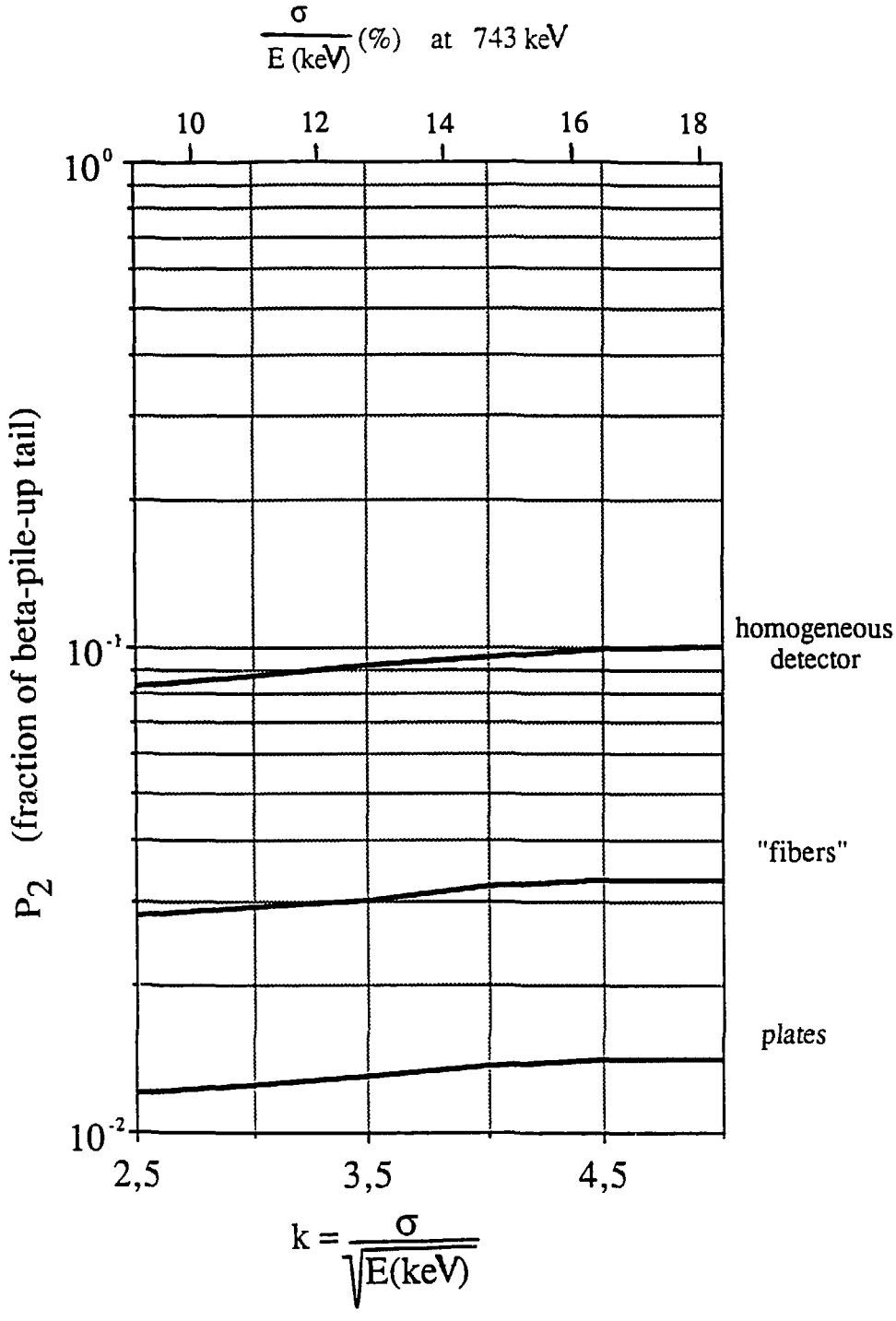

Fig. 5.1 The proportion p_2, of pile-up events, from indium β-decay, which fall in the energy window 660 to 880 keV, is plotted as a function of the energy resolution parameter $k=\sigma/\sqrt{E}$ for 3 types of detectors: homogeneous indium loaded liquid scintillator, thin indium plates (40 mg/cm^2) associated with scintillators, and 1 mm diameter scintillating fibers coated with 10% of indium (2.6 mg/cm^2). The resolution σ/E (%) at 743 keV (the e^- energy from ^{7}Be neutrino interactions) is shown on the upper horizontal scale.

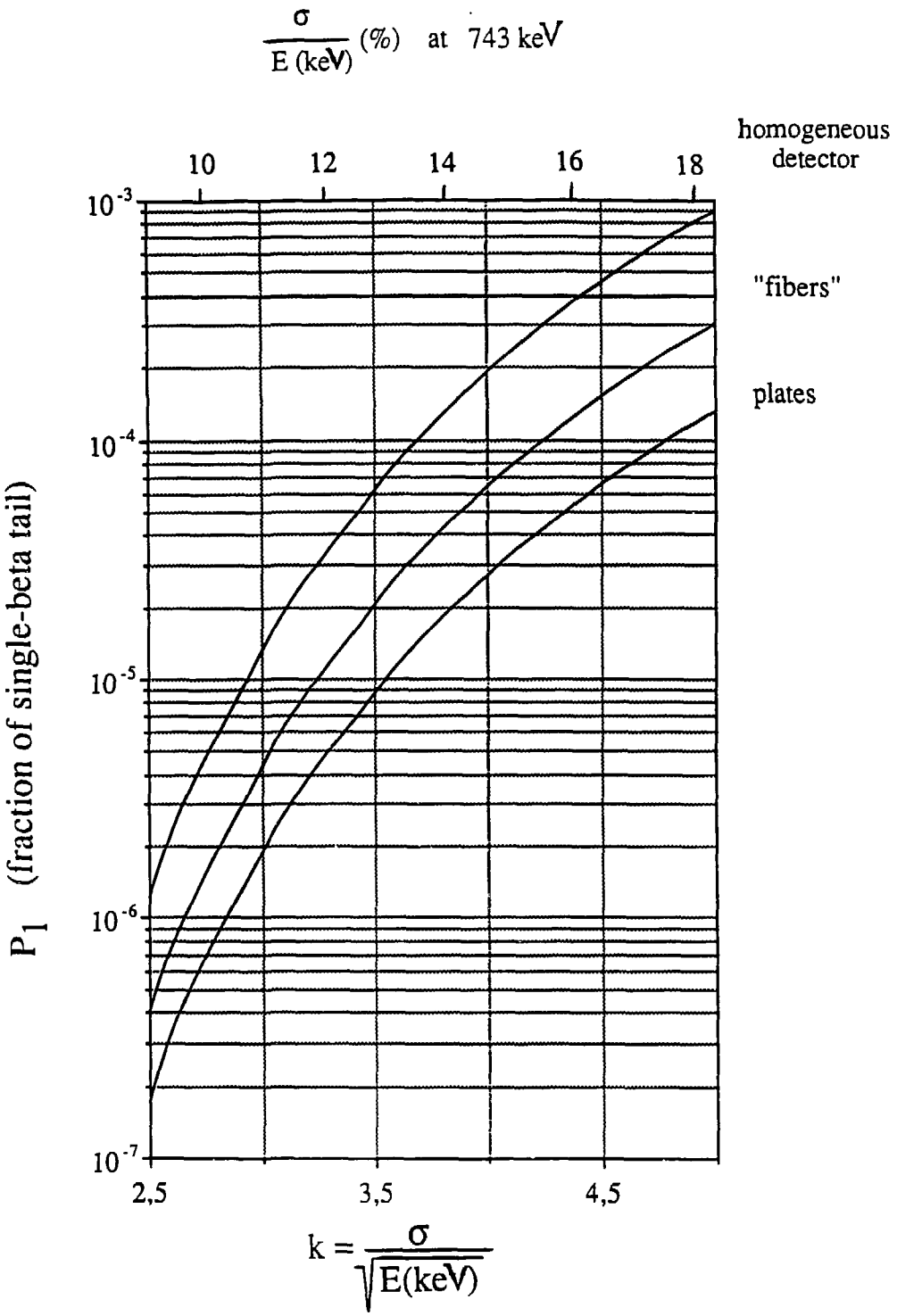

Fig. 5.2 The proportion, p_1, of single β events from indium decay, which fall in the energy window 660 to 880 keV, is plotted as a function of the energy resolution parameter $k=\sigma/\sqrt{E}$ for 3 types of detectors: homogeneous indium loaded liquid scintillator, thin indium plates (40 mg/cm^2) associated with scintillators, and 1 mm diameter scintillating fibers coated with 10% of indium (2.6 mg/cm^2). The resolution σ/E (%) at 743 keV (the e^- energy from ^{7}Be neutrino interactions) is shown on the upper horizontal scale.

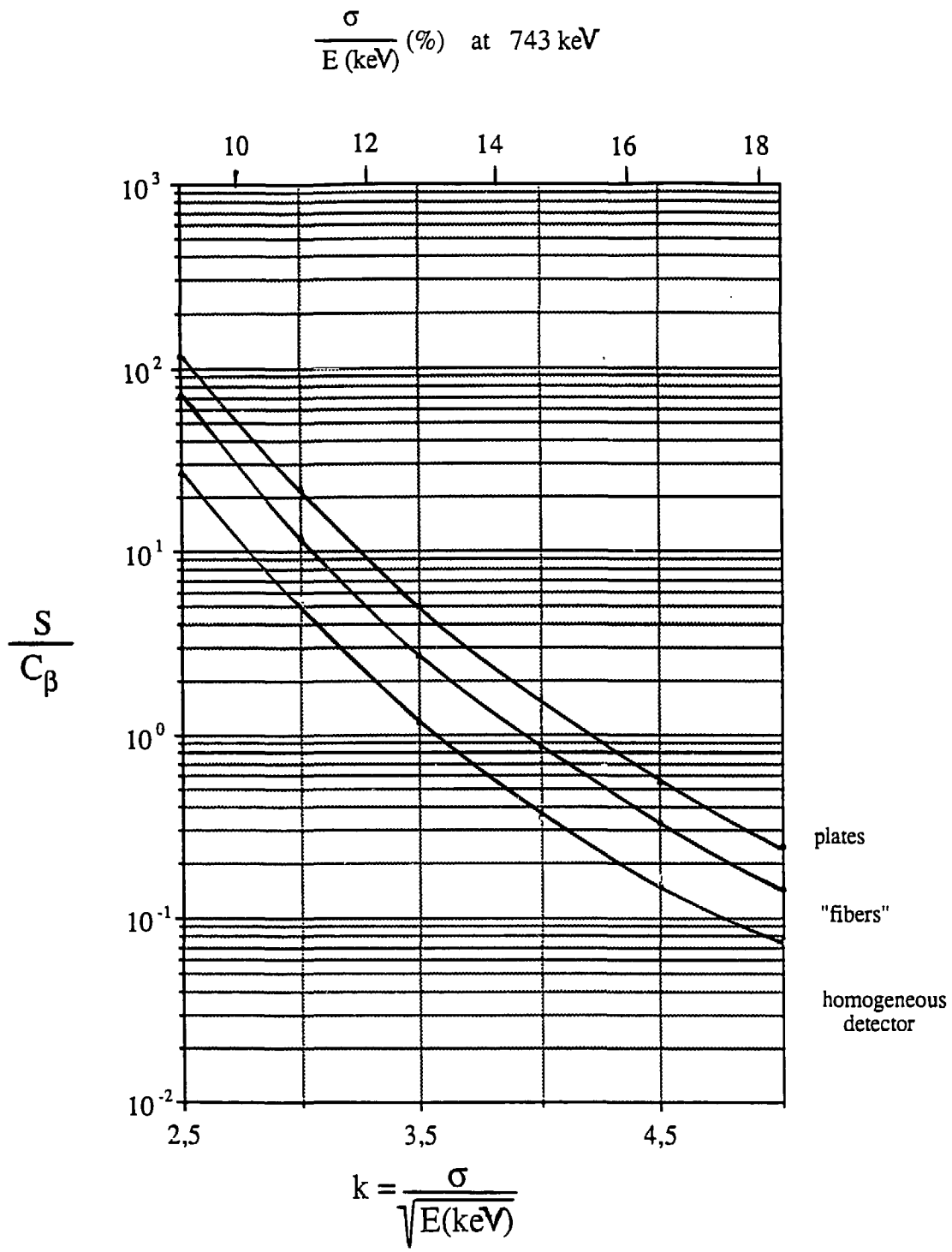

Fig. 5.3 The ratio S / C_β of the solar ν_e signal from ^7Be to the rate C_β of random β-type coincidences, within 10 μs (see Table 5.1), is given as a function of the energy resolution parameter $k=\sigma/\sqrt{E}$ for 3 types of detectors : homogeneous indium loaded liquid scintiliator, thin indium plates (40 mg/cm^2) associated with scintillators, and 1 mm diameter scintillating fibers coated with 10% of indium (2.6 mg/cm^2). The resolution σ/E (%) at 743 keV (the e^- energy from ^7Be neutrino interactions) is shown on the upper horizontal scale.

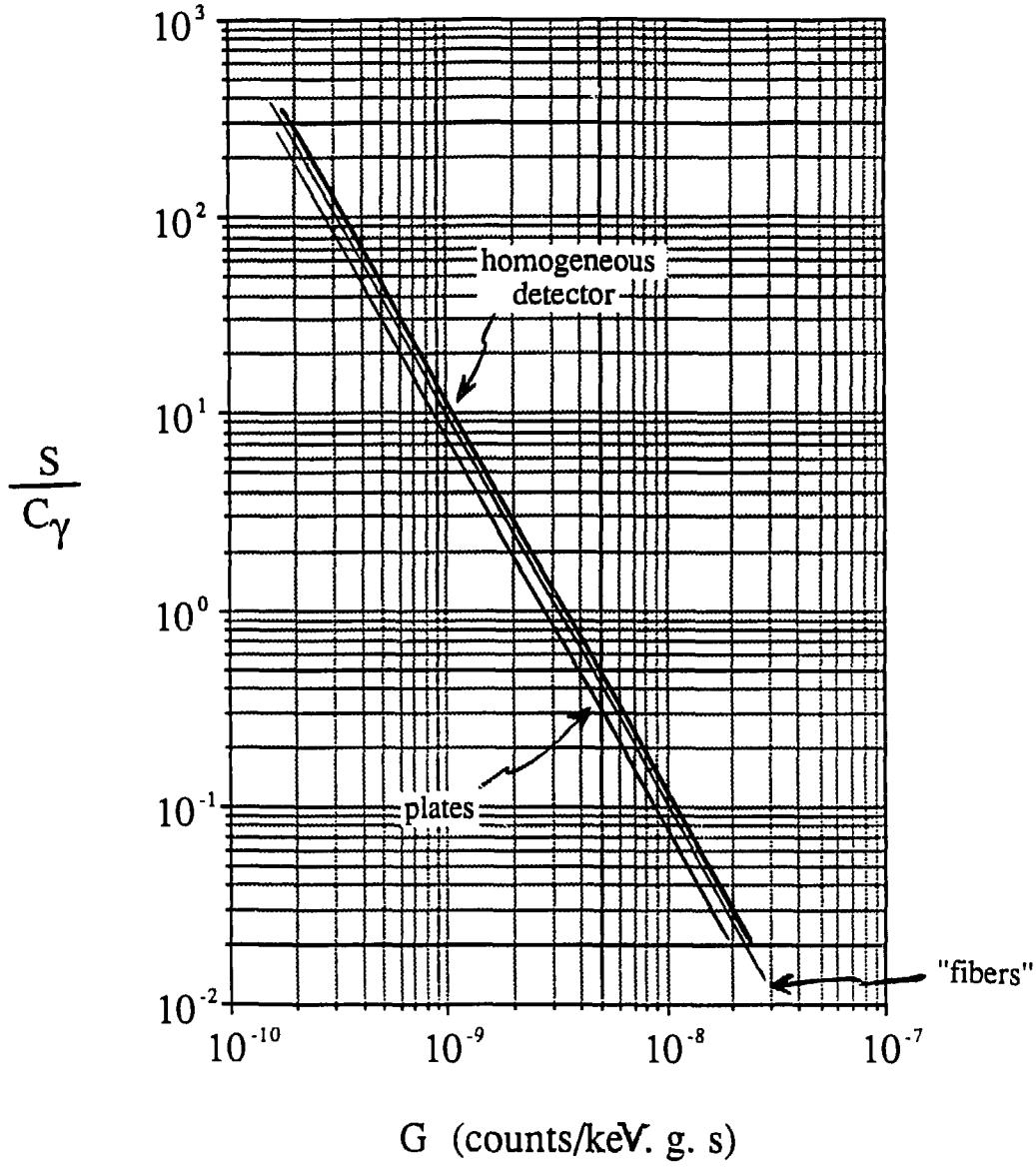

Fig. 5.4

The ratio S / Cγ of the solar ν_e signal from ^{7}Be to the rate C_γ of random γ-type coincidences, within 10 μs (see Table 5.1), is given as a function of the γ-background rate G (expressed in units of $keV^{-1}g^{-1}sec^{-1}$) for 3 types of detectors : homogeneous indium loaded liquid scintillator, 1 mm diameter scintillating fibers coated with 10% of indium (2.6 mg/cm^2) and thin indium plates (40 mg/cm^2) associated with scintillators.

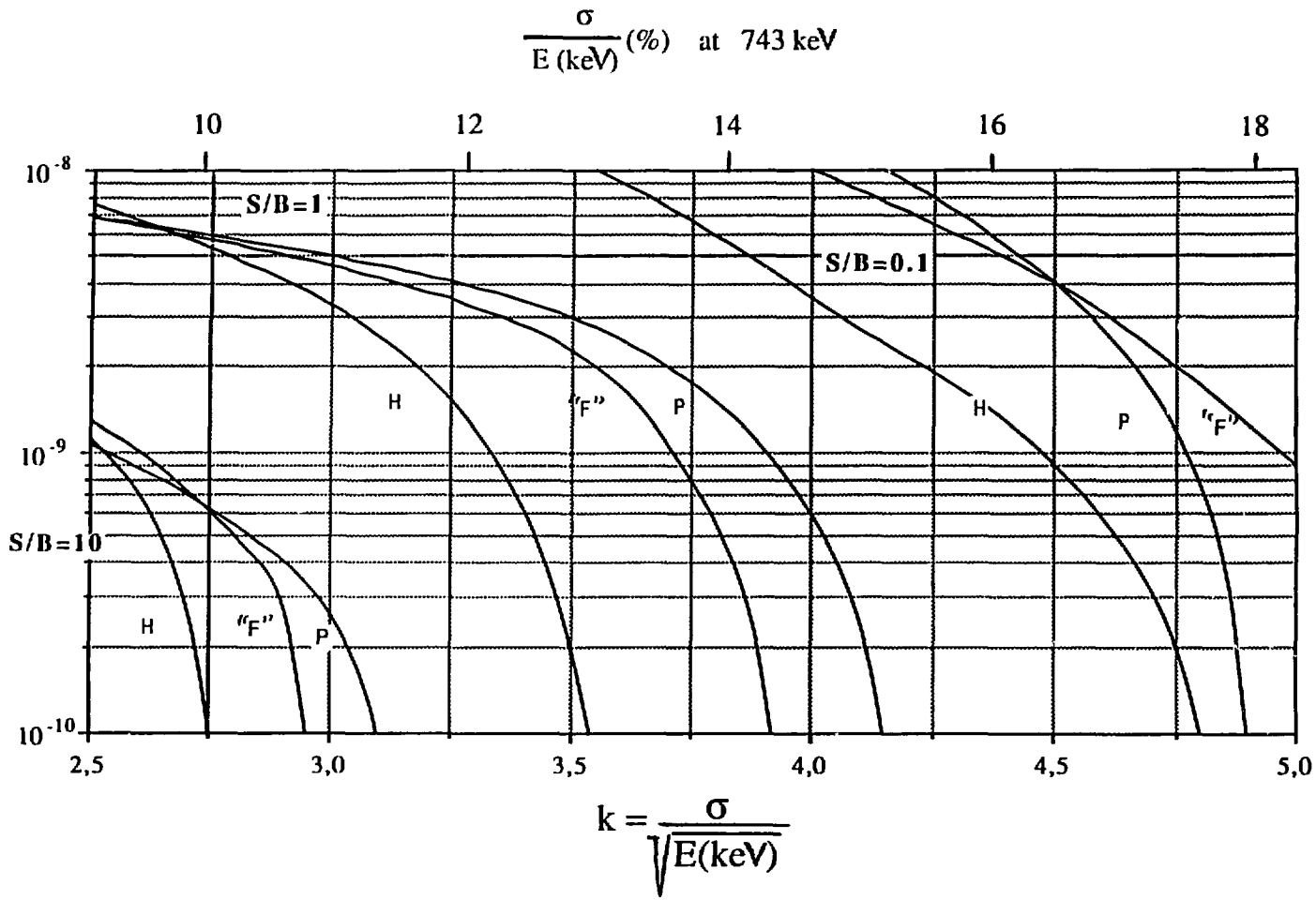

Fig. 5.5 The two main parameters which affect the feasibility of the experiment are shown in a two-dimensional diagram: $k=\sigma/\sqrt{E}$ is the experimental energy resolution; G is the γ-ray background rate in units of g^{-1} sec^{-1} keV^{-1}. Curves are shown for S/B=0.1, 1. and 10. where S is the signal from ^{7}Be neutrinos, and B the total background (β and γ).Results are given for 3 types of cells: homogeneous indium loaded liquid scintillator (**H**), thin indium plates (40 mg/cm^2) associated with scintillators (**P**), and 1 mm diameter scintillating fibers coated with 10% of indium (2,6 mg/cm^2) (**"F"**). The resolution σ/E (%) at 743 keV (the e^- energy from ^{7}Be neutrino interactions) is shown on the upper horizontal scale.The diagram shows that for S/B ≥1, the energy resolution must be 10-12 % and the γ background G below a few 10^{-9} g^{-1} sec^{-1} keV^{-1}.

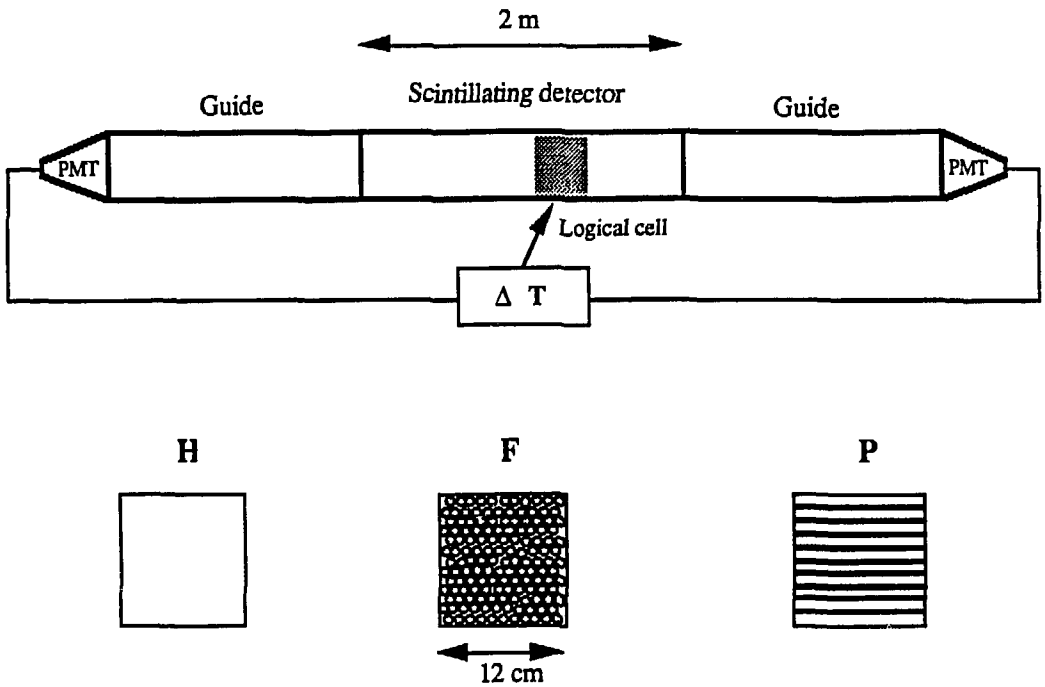

Fig. 6.1 Schematic drawing of a physical cell showing the active scintillating detector, the light guides to the photomultiplier tubes (PMT), and the division into logical cells through time measurement. Also shown are sketches of the cross section of the cell for the three detector types considered: homogeneous indium loaded liquid scintillator (**H**), 1 mm diameter scintillating fibers coated with 10% of indium (2,6 mg/cm^2) (**F**), and thin indium plates (40 mg/cm^2) associated with scintillators (**P**).